ORIGINAL RESEARCH

Aerobic Capacity and Exercise Mediate Protection Against Hepatic Steatosis via Enhanced Bile Acid Metabolism

Benjamin A. Kugler[1,2,†], Adrianna Maurer[1,†], Xiaorong Fu[3], Edziu Franczak[1,2], Nick Ernst[1], Kevin Schwartze[1], Julie Allen[1], Tiangang Li[4], Peter A. Crawford[5], Lauren G. Koch [6], Steven L. Britton[7], Kartik Shankar[8], Shawn C. Burgess[3,*], John P. Thyfault [1,2,9,10,*]

[1]Departments of Cell Biology and Physiology, Kansas Medical Center, Kansas City, KS, 66160, USA, [2]Division of Endocrinology and Clinical Pharmacology, Department of Internal Medicine, KU Diabetes Institute, Kansas Medical Center, Kansas City, KS, 66106, USA, [3]Center for Human Nutrition and Department of Pharmacology, University of Texas Southwestern Medical Center, Dallas, TX, 75390, USA, [4]Department of Biochemistry and Physiology and Harold Hamm Diabetes Center, University of Oklahoma Health Sciences Center, Oklahoma City, OK, 73104, USA, [5]Division of Molecular Medicine, Department of Medicine, and Departments of Biochemistry, Molecular Biology, and Biophysics, University of Minnesota, Minneapolis, MN, 55455, USA, [6]Department of Physiology and Pharmacology, The University of Toledo, Toledo, OH, 43614, USA, [7]Department of Anesthesiology, University of Michigan, Ann Arbor, MI, 48109, USA, [8]USDA Agricultural Research Service, Responsive Agricultural Food Systems Research Unit, College Station, TX, USA, [9]Kansas Center for Metabolism and Obesity Research, Kansas Medical Center, Kansas City, KS, 66160, USA, [10]Kansas City VA Medical Center, Kansas City, 64128, MO

*Address correspondence to J.P.T. (e-mail: jthyfault@kumed.edu), S.C.B. (e-mail: shawn.burgess@utsouthwestern.edu)
†Co-First Authors.

Abstract

High cardiorespiratory fitness and exercise show evidence of altering bile acid (BA) metabolism and are known to protect or treat diet-induced hepatic steatosis, respectively. Here, we tested the hypothesis that high intrinsic aerobic capacity and exercise both increase hepatic BA synthesis measured by the incorporation of ^2H_2O. We also leveraged mice with inducible liver-specific deletion of *Cyp7a1* (LCyp7a1KO), which encodes the rate-limiting enzyme for BA synthesis, to test if exercise-induced BA synthesis is critical for exercise to reduce hepatic steatosis. The synthesis of hepatic BA, cholesterol, and *de novo* lipogenesis was measured in rats bred for either high (HCR) or low (LCR) aerobic capacity consuming acute and chronic high-fat diets. HCR rats had increased synthesis of cholesterol and certain BA species in the liver compared to LCR rats. We also found that chronic exercise with voluntary wheel running (VWR) (4 weeks) increased newly synthesized BAs

of specific species in male C57BL/6J mice compared to sedentary mice. Loss of *Cyp7a1* resulted in fewer new BAs and increased liver triglycerides compared to controls after a 10-week high-fat diet. Additionally, exercise via VWR for 4 weeks effectively reduced hepatic triglycerides in the high-fat diet-fed control male and female mice as expected; however, exercise in LCyp7a1KO mice did not lower liver triglycerides in either sex. These results show that aerobic capacity and exercise increase hepatic BA metabolism, which may be critical for combatting hepatic steatosis.
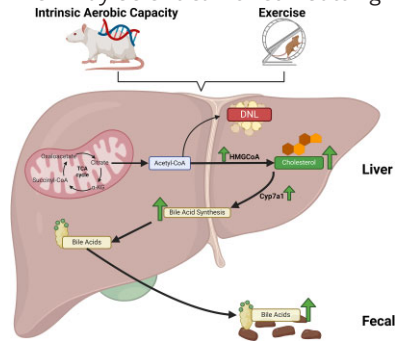
Key words: liver; metabolism; cholesterol synthesis; de novo lipogenesis; metabolic associated steatotic liver disease; Cyp7a1

Introduction

Metabolic dysfunction-associated steatotic liver disease (MASLD) is a global epidemic that is associated with metabolic comorbidities.[1] MASLD encompasses a spectrum of liver diseases that begin with the excess accumulation of liver fat ($\geq$5% of liver weight) and can progress to metabolic-associated steatohepatitis with inflammation and liver injury. Without intervention, MASLD can lead to irreversible fibrosis (ie, cirrhosis) and an increased risk of liver cancer (ie, hepatocellular carcinoma).[2] Although pharmaceutical treatments for MASLD continue to be evaluated, lifestyle modifications, primarily exercise and dietary changes, remain first-line interventions. In humans, aerobic exercise training improves aerobic capacity (ie, cardiorespiratory fitness) while reducing liver triglycerides,[3] which is recapitulated in rodent models.[4] Importantly, the effect of aerobic exercise training to combat hepatic steatosis occurs without weight loss. In addition, lower aerobic capacity independent of body weight has been reported to be associated with MASLD in humans and rodent models.[5–8] However, the mechanisms by which aerobic capacity and aerobic exercise training prevent and treat hepatic steatosis remain largely unknown.

Elevated fatty acids released from adipose tissue and diet, greater hepatic de novo lipogenesis (DNL) from carbohydrates/glucose, and reduced metabolism of fatty acids (fat oxidation, FAO) have all been implicated as causes of MASLD.[9] Utilizing rats bred over several generations for intrinsic aerobic capacity differences, we have shown that high-capacity runners (HCR) have higher hepatic mitochondrial oxidative capacity (ie, FAO) and are protected from MASLD after exposure to both an acute or chronic high-fat diet (HFD).[6–8] However, low-capacity runner rats, with their reduced intrinsic aerobic capacity and lower hepatic oxidative capacity, are highly susceptible to developing steatosis induced by acute and chronic HFD. Our recent findings demonstrate that HCR rats have elevated gene expression in the cholesterol and bile acid synthesis pathway (ie, *Hmgcr* and *Cyp7a1*) and increased fecal bile acid loss compared to LCR rats.[10,11] In addition, aerobic exercise training was shown to increase fecal bile acid loss in LDL receptor (*Ldlr*) knockout mice.[12] Further, bile acid sequestrants and the overexpression of cholesterol 7α-hydroxylase (*Cyp7a1*), the rate-limiting enzyme in bile acid synthesis, also increase fecal bile acid loss and

protect rodents from steatosis and metabolic derangements of diet-induced obesity.[13–15] Elevated hepatic free cholesterol levels are observed in patients with MASLD, and animal models have confirmed the role of increased hepatic free cholesterol in promoting MASLD progression.[16,17] Because cholesterol is a substrate for bile acid metabolism, increases in bile acid synthesis combined with increased fecal bile acid loss and overall bile acid turnover could lower cholesterol. In fact, fecal loss of cholesterol and bile acid is the sole method of cholesterol elimination. However, it is unclear if aerobic capacity and exercise training directly upregulates bile acid synthesis and if this is critical for the benefits of exercise in treating MASLD. Thus, we hypothesize that high aerobic capacity and aerobic exercise training exert their protection against MASLD by promoting bile acid synthesis.

Total bile acid concentration can be quantified by enzymatic assay or by modern liquid chromatography-tandem mass spectrometry (LC-MS/MS), while inference of bile acid synthesis most commonly relies on surrogates of CYP7A1 enzyme activity, such as 7-hydroxy-4-cholesten-3-one (C4). Here, we used a deuterated water (^2H_2O) tracer, which is commonly used to determine the fractional synthesis of lipids, including sterols,[18–26] and analogous assumptions have been applied to bile acid synthesis using ^3H_2O.[27] Fractional bile acid, cholesterol, and lipid synthesis were quantified in sedentary HCR and LCR rats provided short-term (1 week) and chronic (20 weeks) HFD. Bile acid synthesis was activated in HCR rats in response to HFD. Moreover, these effects were recapitulated by chronic exercise training (via voluntary wheel running (VWR)) in mice. We further found that inducible liver-specific *Cyp7a1* knockout mice had lower bile acid synthesis and were resistant to the effects of aerobic exercise training (VWR) to reduce liver triglycerides, suggesting that exercise training-induced bile acid synthesis is critical for the beneficial effects of exercise that treats or protects against steatosis.

Materials and Methods

Ethical Approval

All protocols were approved by the Institutional Animal Care and Use Committee at the University of Kansas Medical Center (KUMC, animal protocol number 2021-2614). All experiments

were carried out following the Guide for the Care and Use of Laboratory Animals published by the National Institutes of Health (NIH Guide, 8th ed., 2011) and adhere to the American Physiological Society's Guiding Principles in the Care and Use of Vertebrate Animals in Research and Training. Male rats and mice were single-housed in a reverse 12 h:12 h, dark: light cycle. For terminal procedures, rats and mice were anesthetized with pentobarbital sodium (100 mg/kg), corresponding to the beginning of the dark cycle.

High-Capacity and Low-Capacity Rat Study

The HCR and LCR rat model was developed and characterized at the University of Toledo as previously described[6–8,28,29] and shipped to KUMC for the study. At 25-30 weeks of age, animals were singly housed (12:12-h light-dark cycle, 24–26°C). Two different sets of HCR and LCR rats were used for the 1-week ($n = 8$) and 20-week ($n = 10$) diet interventions. Only male rats were used in these studies, as females do not develop hepatic steatosis on HFD.

During the 1-week study, 64 male rats (32 HCRs, 32 LCRs) were acclimatized to the control low-fat diet (LFD; D12110704: 10% kcal fat, 3.5% kcal sucrose, and 3.85 kcal/g, Research Diets, New Brunswick, NJ) for at least 2 weeks before half of each LCR and HCR group ($n = 16$) were transitioned to a high-fat diet (D12451: 45% kcal fat, 17% kcal sucrose, and 4.73 kcal/g, Research Diets). The other half remained on LFD for 1 week. On the evening before the termination of the experiment at 5 PM, rats were given intraperitoneal ^2H_2O (DLM4-1, Cambridge Isotope Laboratories, Inc., Andover, MA) injections at a dose of 15 μL/g. This dose was estimated to enrich body water to ~4% ^2H_2O. After dosing, rats were subsequently provided 4% ^2H_2O drinking water for the remainder of the experiment. Half of the rats from each group in the 1-week study were fasted overnight (~4 PM-8 AM) (FASTED), while the remaining animals had access to food (FED), allowing us to determine metabolic effects (ie, DNL, cholesterol synthesis, and bile acid synthesis) of feeding status across strains ($n = 8$ per group). The measurements of food intake, body mass, and body composition (MRI model 900; EchoMRI, Houston, TX) were taken before and after the 1-week intervention. Rats were placed in clean cages just prior to the 1-week diet intervention, and all fecal matter was collected from each cage at the end of the 1-week study.

For the 20-week study, 40 rats (20 HCR, 20 LCR) were acclimated to a control low-fat diet (LFD) for at least 2 weeks and then randomly assigned to either continue on the LFD or switch to an HFD for 20 weeks ($n = 10$ per group). All rats had *ad libitum* access to food until euthanasia. Food consumption was measured weekly and averaged over the 20-week intervention. Body mass and composition were measured before and after the 20-week intervention. Similar to the 1-week study, rats received an intraperitoneal injection of ^2H_2O the evening before (~5 PM) euthanasia and were provided with 4% ^2H_2O drinking water for the remainder of the study. Tissue processing and euthanasia for both the 1-week and 20-week studies were conducted between 10 am (start of the dark cycle) and concluded before 11:30 AM. Immediately following euthanasia, blood, liver, and small intestine samples were collected. A segment of the small intestine, from the duodenum to the beginning of the ileum, was excised, and the luminal contents were removed. Tissues were snap-frozen in liquid nitrogen and stored at −80°C. Blood samples were kept on ice for 30 min, then centrifuged at 7000 × g for

10 min at 4°C. The resulting serum was collected and stored at −80°C.

Mouse Voluntary Wheel Running Study

Male C57Bl/6J mice (10-12 weeks old; The Jackson Laboratory) were singly housed near thermoneutrality (12:12-h reverse light-dark cycle; ~30°C) with *ad libitum* access to water and food. Half of the mice were provided with voluntary running wheels (VWR) for 4 weeks, while the other half were maintained in a sedentary condition ($n = 8$ per group). During the intervention, all mice were on an HFD. To eliminate acute exercise as a confounding variable, running wheels were removed from the hub and placed on the side in VWR cages 24 h prior to tissue collection. Tissue and serum collection were conducted as described for the rat study and were conducted between 10 AM (start of the dark cycle) and concluded prior to 11:30 AM. The administration of ^2H_2O occurred at ~5 PM the night before termination. Mice were only euthanized in the fed condition.

Liver-Specific *Cyp7a1* Knockout Study

At 10-14 weeks of age, male and female C57BL/6J mice with floxed exons 2-4 of the *Cyp7a1* gene (*Cyp7a1*^{fl/fl}, GenePharmatech, Cambridge, MA, T009224) were singly housed at thermoneutrality (12:12-h reverse light-dark cycle; ~30°C) with *ad libitum* access to an HFD to induce hepatic steatosis. After 4 weeks on the HFD, *Cyp7a1*^{fl/fl} mice were randomly assigned to receive either an intraperitoneal injection of control adeno-associated virus 8 (AAV8)-thyroxin-binding globulin promoter (TBG)-GFP (Control, Ctrl) or AAV8-TBG-Cre leading to liver-specific *Cyp7a1* knockout (LCyp7a1KO). Two weeks post-injection, mice either remained sedentary (SED) or were given access to VWR for daily exercise for 4 weeks to treat hepatic steatosis, resulting in 4 groups: Ctrl/SED, Ctrl/VWR, LCyp7a1KO/SED, and LCyp7a1KO/VWR ($n = 6$-8 per group in both males and females). To eliminate acute exercise as a confounding variable, running wheels were removed from the hub and placed on the side in VWR cages 24 h prior to tissue collection. Tissue and serum collection were performed as described for the rat study, including administration of ^2H_2O the night before termination at 5 PM. In addition, a small portion of fresh liver tissue was fixed in 10% formalin, embedded in paraffin, and sectioned. Hematoxylin and eosin staining was performed to visualize intrahepatic lipid content. All mice were euthanized in the fed state.

Body Composition Analysis

Body composition and body mass were measured as previously described on the day of tissue collection.[8,30] Body composition was determined by quantitative magnetic resonance imaging using an EchoMRI-1100 (EchoMRI, TX). Fat-free mass (FFM) was calculated as the difference between body weight and fat mass (FM).

Intestine and Fecal Total Bile Acids

The small intestine was frozen and powdered under liquid nitrogen. Rats and mice within the LCyp7a1 VWR study received fresh cages 7 days prior to euthanasia, and a total of 7 days of fecal excretion was collected from individual cages. For the rat study, due to the 7-day collection period and the short duration of the overnight fast, fecal samples represent a combination of both

fed (6 days) and fasted states (1 night). Intestinal tissue (100 mg) and feces (100 mg) were weighed, then homogenized using a TissueLyzer II (Qiagen, Germantown, MD) bead homogenizer in 1 mL of 100% EtOH. Samples were sealed in parafilm and heated overnight at 50°C, then centrifuged at 1635 × *g* for 20 min. The supernatant was used to measure total bile acid concentration with a commercially available colorimetric kit (DZ042A-KY1/-CAL; Diazyme Laboratories, Inc., Poway, CA). To account for total bile acid content, bile acid concentration was multiplied by total intestinal or fecal weight (from a 1-week collection). Intestinal and fecal bile acid values were corrected for body weight to control for significant differences in body mass.

Fecal Energy Measurements

Homogenized fecal matter was weighed and pressed into pellets using a Pellet Press (∼600 mg) (2811; Parr Instruments, Moline, IL). RO water (2 L) was weighed out to 2000 g ± 0.5 g in a calorimetry bucket (A391DD; Parr Instruments, Moline, IL), then placed into a 6100 Compensated Calorimeter (6100EA; Parr Instruments, Moline, IL). Fecal pellets were weighed to 0.0001 g and placed into a fuel capsule (43AS; Parr Instruments, Moline, IL). An ignition thread (845DD; Parr Instruments, Moline, IL) was tied to the fuse wire of an Oxygen Combustion Vessel (1108P; Parr Instruments, Moline, IL) before placing the pellet-fuel capsule into the vessel and sealing it. An oxygen supply was connected to the vessel's inlet valve and then filled to the recommended pressure of 450 psig. After the vessel was pressurized with oxygen, the ignition wires of the calorimeter were connected to the vessel before being placed into the water-filled calorimetry bucket in the calorimeter. The sample ID and mass were entered into the calorimeter prior to starting the system. To account for total energy content, energy concentration was multiplied by total fecal weight (from a 1-week collection) and corrected for body weight.

Serum Biological Assay

Serum alkaline phosphatase (ALP), aspartate aminotransferase (AST), alanine aminotransferase (ALT), albumin, total protein, blood urea nitrogen (BUN), cholesterol, glucose, and triglyceride measurements were analyzed by a commercial laboratory, IDEXX BioAnalytics (North Grafton, MA). Serum β-hydroxybutyrate was determined using a commercially available kit (2440-058; EKF Diagnostics, Boerne, TX). Serum non-esterified fatty acids (NEFAs) were determined using a commercially available kit (NC9517308, −09, −10, −11, −12; FUJIFILM Medical Systems, USA). Serum insulin was determined using a commercially available ELISA kit (80-INSRT-E01; ALPCO, Salem, NH).

Gene Expression Analysis

RNA was extracted using RNeasy Mini Kit following the manufacturer's instructions (74 104; Qiagen, Hilden, DE). Liver gene expression profiles were assessed via bulk RNA sequencing as previously described.[31] Isolation of polyA RNA and construction of barcoded RNA-seq libraries were performed using TruSeq reagents according to manufacturer's protocols (Illumina). Quantification of the RNAseq libraries was done using Qubit dsDNA high sensitivity reagents, diluted, denatured, and sequenced using Illumina methodology (HiSeq 2500, 50 bp single reads). Following sequencing and demultiplexing, reads were trimmed for adapters, filtered based on Phred quality score, and

aligned to the rat genome using the STAR aligner. Resulting .bam files were imported in SeqMonk for gene-level quantification. Differential expression was conducted with functions in the limma package, and analysis, including PCA, was performed using functions in base R. Plotting was done using the ggpubr package. RNA-seq quality metrics, including the proportion of reads aligning to genic regions, were calculated. Pairwise comparisons between HCR and LCR groups within each diet type were performed, and differentially expressed genes were identified ($P < .05$ and minimum + 2-fold change). Multiple testing corrections were done using the FDR method. Additional analyses were performed using packages in the R statistical software, ShinyGO app, and Gene Set Enrichment Analysis Java application (Broad Institute).

For the Cyp7a1KO study, hepatic RNA and cDNA were prepared as previously described.[10] Real-time quantitative PCR was performed utilizing Prism 7000 and SYBR green primer for Cyp7a1. Gene expression was normalized to peptidylprolyl isomerase B (PPIB) and expressed as fold change compared with the HCR control group.

Serum Bile Acid Profiling by LC-MS/MS

Serum bile acid concentrations were quantified by the University of Oklahoma, Laboratory for Molecular Biology and Cytometry Research Metabolomics Core (Oklahoma City, OK) using LC-MS methodology as performed previously.[32] 300 μL of serum was thawed then vortexed with 600 μL of methanol (MeOH) and incubated on ice for 1 h to precipitate protein. The mixture was centrifuged at 15 000 × *g* at 4°C for 20 min. Supernatant was transferred to a new Eppendorf tube and dried with Speed-Vacuum. Samples were resuspended in 200 μL of acetonitrile/H_2O (30:70, v/v) with 0.1% formic acid, including 100 ng/mL of d8-glycochenodeoxycholic acid as internal standard, sonicated for 10 min in water bath, and the supernatant (100 μL) was used for MS analysis.

Tissue Bile Acid Concentration and ^{2}H Enrichment Measured by LC-MS/MS

BA detection was based on a previously reported method with modification.[33–36] Briefly, 10 μL of 0.1 μg/μL d9-taurochenodeoxycholic acid (d9-TCDCA) internal standard was added to the liver tissues (approximately 30 mg), and the tissue was finely homogenized in 500 μL ice cold MeOH/H_2O (85:15, v/v) in a 2.0-mL pre-filled Bead Ruptor Tubes (2.8 mm ceramic beads, Omni International, Kennesaw, GA, USA). After centrifugation (1635 × *g* for 10 min) to precipitate the proteins, the supernatant was transferred to a new tube and dried under N_2. To the dried samples, 150 μL of MeOH/H_2O (50:50, v/v) with 0.1% formic acid was added before MS analysis.

LC-MS/MS chromatographic separation of bile acids was performed using a reverse phase C8 column (Phenomenex Luna C8, 150 × 2.0 mm, 3 μm) at a flow rate of 0.2 mL/min. The mobile phase consisted of MeOH/H_2O (2:98, v/v) with 0.0125% acetic acid (eluent A) and ACN/H_2O (95:5, v/v) with 0.1% formic acid (eluent B). The gradient proceeded from 25% to 40% B over 12 min and then 40%–75% B over 12 min. The column was washed with 100% B for 10 min and equilibrated with 25% B for 10 min between injections. Bile acids were detected by an API 3200 triple-quadrupole LC-MS/MS (AB Sciex, MA) operated in negative ionization mode. The ion source parameters were set as follows: curtain gas: 20 psi, ion spray voltage: −4000 V, ion source temperature: 300°C, and nebulizing and drying gas: 30 and 40 psi. The

MS/MS system was operated in multiple reaction monitoring (MRM) mode, and MRM transition for each compound were automatically set up by direct infusion of each individual standard. The declustering potential, collision energy, entrance potential, and cell exit potential were −120 V, −120 V, −10 V, and −8 V. An m/z value of 80 (SO_3^- anion from the taurine moiety) was selected as the common product ion for all the taurine conjugates, tauro-α-muricholic acid (TαMCA), tauro-β-muricholic acid (TβMCA), taurocholic acid (TCA), tauro-chenodeoxycholic acid (TCDCA), and tauro-deoxycholic acid (TDCA). Mass to charge (m/z) values of 498.2 (TCDCA and TDCA), 514.2 (TMCA and TCA), and 507.2 (d9-TUDCA) were selected as precursors. MRM transitions for m0, m1, m2, m3 mass isotopologues of deuterated TαMCA, TβMCA, TCA, TCDCA, TDCA, and d9-TCDCA internal standard are summarized in Table S1. Given the existence of isobaric structures in the bile acid pool, we optimized reverse phase LC detection against a mixture of bile acids as reported by Han et al.[37] Structural isomers, TαMCA, TβMCA, and TCA, share the same MRM transitions but were chromatographically separated. TUDCA, TCDCA, and TDCA isomers were also baseline-separated (Figure S1). Calibration curves were constructed with a fixed amount of d9-TCDCA internal standard. Values for the slope, intercept, and correlation coefficient were obtained by linear-regression analysis of the calibration curves. The area under each analyte peak, relative to the internal standard, was used to calculate the analyte concentrations in liver samples.

Liver Cholesterol Concentration and ^{2}H Enrichment Measured by HR-Orbitrap-GCMS

Approximately 20 mg of tissue was weighed and homogenized with 1 mL of MeOH/dichloromethane (DCM) (1:1, v/v) in 2.0-mL pre-filled Bead Ruptor Tubes. Tubes were washed twice with 1 mL MeOH/DCM, and all solutions were combined. Samples were vortexed and then centrifuged for 5 min at 1635 × g. 50 μL of 0.05 μg/μL d7-cholesterol was added to 2 mg of supernatant and dried under N_2. Dried extracts were saponified with 1 mL of 0.5 M KOH in MeOH at 80°C for 1 h. Lipids were extracted with DCM/water before evaporation to dryness. The dried lipid extract was derivatized by incubation at 75°C for 1 h with 100 μL acetyl chloride. The sample was evaporated to dryness under N_2 and was reconstituted in 100 μL iso-octane for analysis by GCMS.

The ^{2}H-enrichment of cholesterol (m0, m1, m2, m3 isotopologues of deuterated cholesterol) was determined using a Q Exactive GC-orbitrap MS (Thermo Scientific). 1 μL of sample was injected onto an HP-5 ms capillary column (60 m × 0.32 mm i.d., 0.25 μm film thickness) in split mode. Helium gas flow rate was set to 13.5 min of 1 mL/min for the initial injection, followed by 0.4 mL/min for 5 min before returning to 1 mL/min. The GC injector temperature was set at 250°C, and the transfer line was held at 290°C. The column temperature was set to 200°C for 1 min and increased by 20°C/min before reaching 320°C over 16 min. Samples were analyzed at 70 eV in EI mode by targeted selected ion monitoring (t-SIM) at 240 000 mass resolution (FWHM, m/z 200). Tuning and calibration of the mass spectrometer were performed using perfluorotributylamine (FC-43) to achieve a mass accuracy of <0.5 ppm. The quadrupole was set to pass ions between m/z 246.24 and 252.24. The Orbitrap automatic gain control target was set to 5e^4 with a maximum injection time of 54 ms. Cholesterol concentration was calculated from the area ratio of the peaks corresponding to cholesterol (m/z 247.242)

and the D7-cholesterol internal standard (m/z 254.286) with full scan mass ranges 240-260 m/z. Extraction of individual high-resolution m/z values representing each isotopomer ion was done using TraceFinder 4.1 (Thermo Scientific) with 4 ppm mass tolerance.

Triglyceride Palmitate Concentration and ^{2}H Enrichment Measured by HR-Orbitrap-GCMS

Liver palmitate was measured as previously reported[20] and followed the same sample preparation as described for cholesterol analysis, except the dried lipid extract was resuspended in 50 μL of 1% triethylamine/acetone and reacted with 50 μL of 1% Pentafluorobenzyl bromide/acetone for 30 min at room temperature. To this solution, 1 mL of iso-octane was added before MS analysis. The ^{2}H-enrichment of palmitate was determined using HR-Orbitrap-GCMS as previously described.[20]

Body Water Enrichment Measured by HR-Orbitrap-GCMS

Serum samples were dissolved in acetone under alkaline conditions directly in the autosampler vial, as previously reported.[20] In brief, 5 μL of serum sample, 2 μL of 10 M sodium hydroxide, and 5 μL of acetone were added to a threaded GC vial. Samples were incubated overnight at room temperature prior to analysis. Calibration standards of known ^{2}H-mol fraction excess were prepared by mixing weighed samples of naturally labeled water and of 99.9% ^{2}H$_2$O. Negative chemical ionization mode (NCI) was used with t-SIM acquisition (m/z 55.5-60.5) and 60 000 mass resolution (FWHM, m/z 200) on the same HR-Orbitrap-GCMS instrument as described previously.[20]

Fractional Synthesis of Palmitate, Cholesterol, and Bile Acids

The fractional synthesis of palmitate, cholesterol, and bile acids was calculated using the following equation:

$$\text{Fractional synthesis} = \frac{\text{Analyte enrichment}}{(\text{Water enrichment} \times n)} \times 100. \quad (1)$$

Palmitate, cholesterol, and bile acid analyte ^{2}H enrichment were determined from mass isotopomers m1 (^{2}H$_1$), m2 (^{2}H$_2$), and m3 (^{2}H$_3$), as described above, and correction for naturally abundant isotopes was made using the MID of a biological sample (collected without ^{2}H$_2$O administration) and a matrix correction algorithm. Analyte ^{2}H enrichment = ^{2}H$_1$ + (^{2}H$_2$ × 2) + (^{2}H$_3$ × 3). N is the number of deuterium exchangeable hydrogens in each analyte and can be experimentally determined from the binomial distribution of their MIDs.[23,26,38] Palmitate was previously found to have $n = 22$.[20] The partial cholesterol fragment (m/z 247) was determined to have $n = 20$, which is proportionally similar to the full cholesterol ion previously reported.[23] Assignment for TaMCA $n = 14$, TbMCA $n = 10$, TCA $n = 14$, TCDCA $n = 18$, TDCA $n = 10$ were made from their MIDs based on the assumption of normal binomial distributions.

Measurement of Liver Triglycerides

Intrahepatic triglyceride (TAG) measurement was performed with methods adjusted from previously described.[6,28] Briefly,

25 mg of liver tissue was homogenized in tissue lysis buffer (50 mM HEPES, 12 mM sodium pyrophosphate, 100 mM sodium fluoride, 10 mM EDTA, 2% SDS). The homogenate was centrifuged at $8000 \times g$ for 10 min at room temperature, and the supernatant was collected. Protein concentration was determined using a Pierce BCA Protein Assay Kit (Thermo Fisher Scientific). For hepatic lipid extraction, 500 μg of protein was mixed with 1 mL of chloroform: methanol: acetic acid (2:1:0.15, v/v/v). The mixture was centrifuged at $1000 \times g$ for 20 min at 4°C. A 500 μL aliquot of the organic phase was collected. The remaining tissue lysate was re-extracted with an additional 1 mL of chloroform: methanol: acetic acid, and centrifuged again at $1000 \times g$ at 4°C. A 750 μL aliquot of the organic phase was collected from this second extraction. The 2 organic extracts (total volume: 1.25 mL) were combined, evaporated to dryness, and reconstituted in a 3:2 (v/v) butanol: Triton X-114 mixture. Hepatic TAG levels were quantified using a commercially available kit (Sigma, TR0100-1KT), and data were expressed as TAG content per milligram of protein.

Statistics

Measurements at 1 week and 20 weeks in the HCR and LCR rats were analyzed independently. Anthropometrics and energy intake are only reported for the FED groups from the 1-week study and were analyzed using 2-way ANOVA (strain × diet) followed by Tukey's multiple comparisons test. A 3-way ANOVA (strain × diet × feeding status [FED or FASTED]) was used to analyze intestinal, liver, and serum bile acids, serum metabolites, DNL, and cholesterol synthesis, followed by Tukey's multiple comparisons test when a significant interaction was observed. All fecal measurements were corrected for body weight due to significant differences in body mass between HCR and LCR rats. FED and FASTED fecal measurements during the 1-week study were pooled together (animals were only fasted 1 night prior to sacrifice while feces were collected over 7 days) according to strain and diet then analyzed using 2-way ANOVA (strain × diet) followed by Tukey's multiple comparisons test. All 20-week measurements, except bile acid synthesis, were analyzed using 2-way ANOVA (strain × diet) followed by Tukey's multiple comparisons test. Bile acid synthesis measurements were analyzed using an unpaired T-test. In wild-type mice studies, comparisons of bile acid synthesis between VWR and sedentary were made via unpaired T-test. LCyp7a1KO was analyzed within sex utilizing 2-way ANOVA (Genotype × VWR). Statistical analyses were performed in Prism 10 (GraphPad Software, San Diego, CA).

Results

HCR Rats Display Less Weight Gain and Changes in Circulating Lipids on an HFD

As expected, body mass and percent FM were greater, while the percent lean mass was reduced in LCR strain at the end of the 1-week than HCR counterparts (main effect of strain, $P < .05$, Table S2). One week of an HFD significantly increased body mass, which was influenced by increases in FM (main effect of Diet, $P < .05$). However, a diet and strain interaction revealed this was driven by the LCR fed an HFD, as they had a significantly greater increase in FM ($P < .05$), which was not observed in the HCR rats fed HFD. This effect was influenced by increased energy intake from the diet (main effect of diet, $P < .05$) by LCR rats on the HFD ($P < .05$), which was not observed in HCR rats.

Serum metabolic data for 1 week are shown in Table S3. The nutritional state (ie, Fed vs. Fasted) affected all variables except serum NEFAs in the 1-week HFD condition (main effect of fasting, $P < .05$). Surprisingly, ALP, AST, and ALT were significantly lower in LCR rats than matched HCR rats (main effect of strain, $P < .05$). Serum cholesterol, triglycerides, and NEFA were higher in LCR compared to HCR rats (main effect of strain, $P < .05$). Serum insulin was generally lower in LCR rats than in HCR counterparts (main effect of strain, $P < .05$). The HFD increased ALP, BUN, and β-hydroxybutyrate while decreasing cholesterol levels (main effect of diet, $P < .05$). However, a strain × diet interaction revealed that HFD increased BUN in LCR while decreasing BUN in HCR ($P < .05$).

In the 20-week HFD study, body mass, and percent FM were greater, while percent lean mass was reduced in the LCR rats compared to HCR rats regardless of diet (main effect of strain, $P < .05$, Table S4). However, a 20-week HFD significantly increased body mass and percent FM and reduced percent lean mass, irrespective of strain (main effect of diet: $P < .05$). Serum levels of ALP, AST, and ALT did not differ between strains. In contrast, serum cholesterol levels were significantly lower in HCR rats compared to LCR rats, regardless of diet (main effect of strain: $P < .05$; Table S5). Serum β-hydroxybutyrate and NEFA levels were significantly elevated in both strains fed an HFD (main effect of diet: $P < .05$). A significant strain × diet interaction was observed for serum triglycerides ($P < .05$). Specifically, serum triglycerides were elevated in HCR rats fed an LFD compared to LCR rats fed LFD. However, in LCR rats, an HFD significantly increased serum triglycerides compared to those fed LFD.

HCR and LCR Rats Display Different Serum and Liver Bile Acid Levels and Composition

One week after diet intervention, serum total bile acids were significantly lower in HCR rats compared to LCR rats, regardless of diet (main effect of strain, $P < .05$, Figure 1A and Table S6). Due to variations in the serum bile acid pool size, conjugated and unconjugated bile acids were analyzed as a percentage of the total serum bile acid pool. Glycine-conjugated bile acids were higher in LCR rats than HCR rats (main effect of strain, $P < .05$, Figure 1A and Table S6). Fasting led to a higher proportion of glycine-conjugated bile acids in the LCR rats ($P < .05$, Figure 1A and Table S6). The ratio of 12α-hydroxylated to non-12α-hydroxylated bile acids was significantly elevated under fasting conditions (main effect of fasting: $P < .05$; Table S6). A trend toward a strain × feeding status interaction ($P = .06$) suggested that changes in LCR rats largely drove this elevation in 12α-hydroxylated/non-12α-hydroxylated in the fasted condition. This suggests fasting in LCR rats either increases classical bile acid synthesis or decreases alternative bile acid synthesis in LCR rats.

Liver bile acid measurements focused specifically on taurine-conjugated bile acids because they comprise the largest proportion of the bile acid pool in rodents. Total liver bile acid concentration was higher in the LCR rats after the 1-week diet intervention (main effect of strain, $P < .05$, Table 1). Specifically, T-αMCA and T-CA concentrations were greater in LCR than HCR counterparts (main effect of strain, $P < .05$, Table 1). However, fasting increased liver bile acid content, particularly T-CA and T-DCA, in both strains (main effect of fasting, $P < .05$, Table 1).
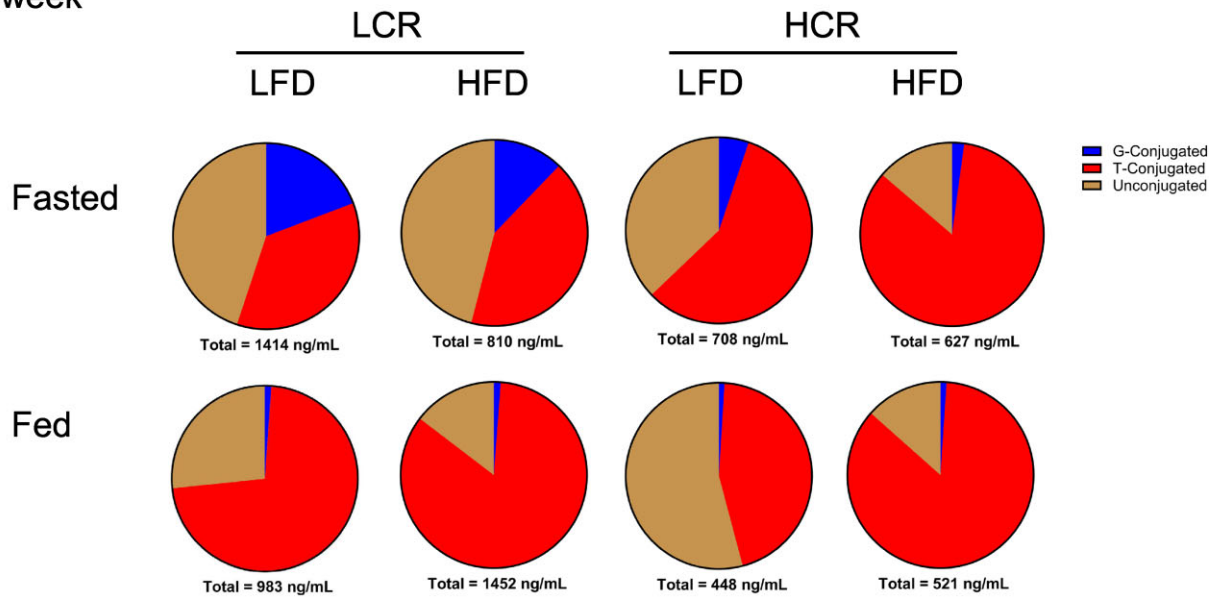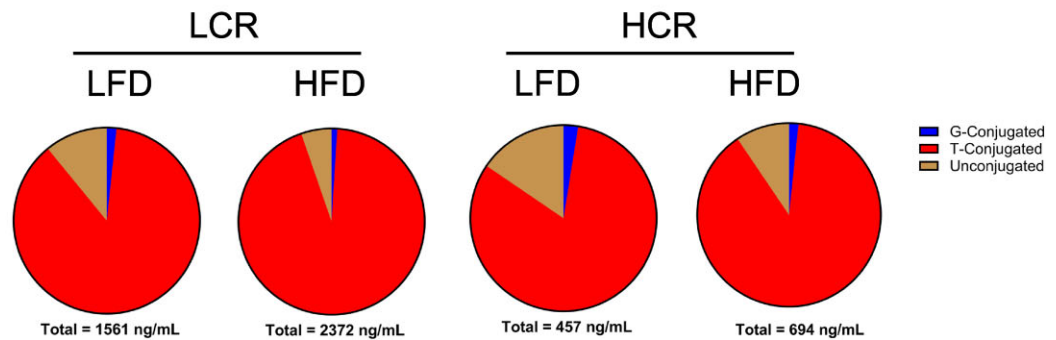
A 1-week

B 20-weeks

Figure 1. Serum bile acid composition. (A) Serum bile acid composition and total bile acids from rats during a 1-week study ($n = 8$). (B) Serum bile acid composition and total bile acids from rats during a 20-week study ($n = 10$).

In the 20-week HFD study, serum bile acid concentration increased in LCR rats but not in HCR (main effect of strain, $P < .05$, Figure 1B and Table S7). This increase was driven by elevated T-βMCA, T-CA, T-DCA, and T-UDCA in LCR (main effect of strain, $P < .05$, Table S7). Again, the 12α-hydroxylated to non-12α-hydroxylated bile acid ratio was higher in LCR rats than in HCR counterparts (main effect of strain, $P < .05$, Table S7); however, regardless of strain, HFD also increased the 12α-hydroxy/non-12α-hydroxy ratio (main effect of diet, $P < .05$, Table S7). Total glycine- and taurine-conjugated bile acids were elevated in LCR rats compared to HCR rats (main effect of strain, $P < .05$, Table S7). Despite these differences, the serum bile acid percent composition was not significantly different between HCR and LCR rats after chronic HFD (Figure 1B). Similar to serum bile acids, liver bile acids were elevated in LCR rats fed an HFD compared to HCR counterparts (main effect of strain, $P < .05$, Table 2) an effect driven by increased T-βMCA and T-CA in LCR (main effect of strain, $P < .05$, Table 2).

HCR Rats Have Increased Fecal Bile Acids and Energy Loss

After correcting for body weight, intestinal bile acids were not different between LCR and HCR rats in either the 1-week or 20-week study (Figure 2A and B). However, fecal bile acid content was significantly higher in HCR rats compared to LCR rats in both diet conditions (main effect of strain, $P < .05$, Figure 2C and D). HCR also had higher fecal energy loss in both diet conditions than LCR (main effect of strain, $P < .05$, Figure 2E and F).

HCR Rats Have Greater Cholesterol and Bile Acid Synthesis

Consistent with our previous findings in mice,[39] a 1-week HFD suppressed DNL compared to LFD in both strains (main effect of diet, $P < .05$, Figure 3A). In the FED state, HCR rats showed a trend toward higher DNL on LFD ($P = .052$; Figure 3A). However, when fed HFD, HCR rats exhibited a significantly greater reduction in DNL than LCR rats in the FED state ($P < .05$, Figure 3B). Hepatic cholesterol synthesis was significantly higher in HCR rats compared to LCR rats (main effect of strain, $P < .05$, Figure 3C), but was significantly reduced during fasting (main effect of fasting, $P < .05$, Figure 3C). DNL and cholesterol synthesis were not measured in the 20-week HFD study.

Newly synthesized bile acids T-CA, T-αMCA, T-βMCA, T-CDCA, and T-DCA were higher in HCR compared to LCR

Table 1. Liver Bile Acid Concentrations From HCR/LCR Rats on an LFD or HFD for 1 Week

(ug/g of liver)	LCR				HCR				P-value					
	FASTED		FED		FASTED		FED							
	LFD	HFD	LFD	HFD	LFD	HFD	LFD	HFD	Strain	Fed	Diet	Strain × Fed	Strain × Diet	Strain × Diet × Fed
T-αMCA	8.2 ± 1.5	7.1 ± 1.4	5.4 ± 0.6	8.3 ± 1.51	5.0 ± 0.6	3.7 ± 0.9	5.9 ± 1.4	4.1 ± 0.8	0.003	0.924	0.721	0.404	0.135	0.173
T-βMCA	13.3 ± 3.2	19.7 ± 9.1	32.3 ± 4.5	35.0 ± 5.1	25.5 ± 3.5	22.2 ± 2.8	19.7 ± 4.0	27.1 ± 6.3	0.696	0.031	0.382	0.023	0.738	0.326
T-CA	112.9 ± 16.7	114.7 ± 22.5	48.6 ± 7.2	71.9 ± 10.2	71.4 ± 9.8	82.3 ± 8.6	29.5 ± 6.1	51.6 ± 10.4	0.002	<0.001	0.091	0.311	0.814	0.768
T-CDCA	10.9 ± 2.6	9.7 ± 1.6	5.6 ± 0.7	10.1 ± 1.6	7.3 ± 1.7	6.8 ± 1.7	8.4 ± 1.6	6.0 ± 0.8	0.077	0.291	0.914	0.251	0.154	0.395
T-DCA	11.5 ± 4.7	9.3 ± 1.9	2.2 ± 0.4	2.3 ± 0.6	10.4 ± 3.1	10.2 ± 0.8	3.2 ± 0.7	2.8 ± 0.5	0.830	<0.001	0.615	0.734	0.781	0.679
TOTAL	156.8 ± 17.6	160.6 ± 34.9	94.1 ± 11.6	127.7 ± 16.9	119.5 ± 13.4	125.2 ± 12.2	66.6 ± 10.0	91.5 ± 17.5	0.009	<0.001	0.184	0.858	0.892	0.838

Values are means ± SEM (n = 6-8).

Table 2. Liver Bile Acid Concentrations From HCR/LCR Rats on Only an HFD for 20 Weeks

(ug/g of liver)	LCR	HCR	P-value
T-αMCA	5.06 ± 0.7	3.14 ± 0.80	.090
T-βMCA	42.24 ± 8.75	17.44 ± 4.90	**.024**
T-CA	118.30 ± 14.52	52.79 ± 9.49	**.001**
T-CDCA	4.08 ± 0.69	3.80 ± 0.74	.781
T-DCA	4.12 ± 0.86	3.56 ± 0.48	.573
TOTAL	173.80 ± 23.90	80.73 ± 15.80	**.005**

Values are means ± SEM (n = 10).

counterparts (main effect of strain, $P < .05$, Figure 3D). Overnight fasting reduced the synthesis of the majority of bile acids except for T-CA, which was increased (main effect of fasting, $P < .05$, Figure 3D). The 1-week HFD reduced bile acid synthesis in both strains and in both fasted/fed conditions (main effect of diet, $P < .05$, Figure 3D). Following the 20-week HFD, the percentage of newly synthesized bile acids was higher in HCR rats than in LCR rats; as primary bile acids T-αMCA, T-βMCA, and T-CA were statistically significant (main effect of strain, $P < .05$, Figure 3E). These data show that elevated bile acid synthesis in HCR over the LCR is maintained over the course of a long term HFD.

Aerobic Capacity Regulates Hepatic Bile Acid Gene Expression

We have previously reported that HCR displays upregulated transcription of cholesterol and bile acid synthesis pathways in the liver than LCR.[10,11] Similarly, HMG-CoA reductase gene (*Hmgcr*) expression was higher in HCR rats (main effect of strain, $P < .05$, Figure 4A) as was gene expression for the rate-limiting enzyme of bile acid synthesis, *Cyp7a1*, and the alternative pathway, *Cyp27a1* (main effect of strain, $P < .05$, Figure 4B and C). Hepatic *Cyp8b1* expression was not different between strains in the 1-week HFD study, but in the fed condition, it was reduced (main effect of fasting, $P < .05$), while the HFD increased expression (main effect of diet, $P < .05$, Figure 4D). Hepatic *Cyp7b1*, which is downstream of *Cyp27a1*, was lower in HCR than LCR across all conditions (main effect of strain, $P < .05$, Figure 4E) as was *Baat* expression, an enzyme that regulates conjugation of bile acids (main effect of strain, $P < .05$, Figure 4F).

Bile acid synthesis is regulated by a negative feedback loop in which bile acids returning to the liver activate the nuclear receptor FXR to suppress *Cyp7a1* expression. Liver FXR (encoded by the *Nr1h4* gene) was lower in HCR rats compared to LCR rats (main effect of strain, $P < .05$, Figure 4G). In contrast, another regulator of bile acid and cholesterol synthesis, *Fgfr4*, was higher in HCR than LCR regardless of diet (main effect of strain, $P < .05$, Figure 4H). Consistent with the differences found for cholesterol synthesis between strains, *Srebp-2* (encoded by the *Srebf-2* gene) expression was consistently higher in HCR vs. LCR (main effect of strain, $P < .05$, Figure 4I). However, a strain and fasting interaction revealed that this difference was driven by lower *Srebp-2* gene expression in fasting LCR rats ($P < .05$). Liver *Srebf-1* expression, which encodes for *Srebp-1*, was induced in both strains in the fed state (main effect of fasting, $P < .05$, Figure 4J) and remained higher in LCR across all diets/conditions (main effect of strain, $P < .05$, Figure 4J). As expected, due to their known higher mitochondrial oxidative capacity, HCR rats had higher hepatic gene expression of the transcriptional co-activator peroxisome gamma co-activator 1 alpha (*Pgc1α*) and peroxisome

proliferator-activated receptor alpha (*Pparα*), regardless of diet or fasting condition (main effect of strain, $P < .05$, Figure 4K and L).

Exercise via VWR Increases Bile Acid Synthesis in Mice

Because exercise can increase aerobic capacity, we next examined whether chronic exercise increases hepatic bile acid metabolism in male mice and recapitulates the contrasting responses in HCR vs. LCR rats. After 4 weeks, VWR increased energy intake but mitigated body weight and FM gain while preserving lean body mass ($P < .05$, Table S8). Remarkably, VWR increased bile acid synthesis by elevating the synthesis of primary bile acids T-CA, T-αMCA, T-βMCA, and T-CDCA, and secondary bile acid T-DCA ($P < .05$, Figure 5A-E) compared to sedentary control mice. These data confirm the induction of bile acid synthesis in response to exercise training.

Cyp7a1 Mediated Bile Acid Synthesis Is Critical for Exercise to Treat Steatosis

We and others have shown that exercise protects and treats HFD-induced hepatic steatosis in mice.[40] In the current and previous studies, we reported that *Cyp7a1* gene expression is upregulated in HCR rats on an HFD and in exercising mice, indicating that *Cyp7a1* may be a critical factor in the ability of exercise to prevent hepatic steatosis.[10,11] We also found that exercise in rats and mice increases hepatic expression of genes regulating bile acid and cholesterol synthesis (*Acly*, *Cyp7a1*, and *Hmgcr*), suggesting that bile acid synthesis is upregulated by exercise.[11] To investigate these effects further, we developed an inducible liver-specific *Cyp7a1* knockout mouse model in which *Cyp7a1* expression was knocked out in the liver before exercise. The LCyp7a1KO had reduced *Cyp7a1* gene expression, confirming the liver-specific knockout of *Cyp7a1* (main effect of LCyp7a1KO, $P < .05$, Figure 6A). Body weight did not differ between genotypes in either male or female mice during the 4 weeks of exercise (Tables S9 and S10). However, as expected, exercise increased daily energy intake (main effect of VWR, $P < .05$, Tables S9 and S10). Male LCyp7a1KO mice exhibited an increase in FFM during the intervention, whereas control males did not (main effect of genotype, $P < .05$, Table S9). Interestingly, female control mice gained FFM, whereas LCyp7a1KO females did not (main effect of genotype, $P < .05$, Table S10). Despite the increased energy intake, exercise mitigated FM gain in both genotypes (main effect of VWR, $P < .05$, Table S10). Overall, liver-specific Cyp7a1 knockout did not significantly alter weight gain but did affect body composition, specifically FFM.

Liver triglycerides (TAGs) were significantly elevated in LCyp7a1KO mice compared to control, regardless of sex or exercise (main effect of LCyp7a1KO, $P < .05$, Figure 6B and C). A significant interaction between VWR and genotype was observed in both sexes ($P < .05$, Figure 6B). Specifically, in female control mice, VWR significantly reduced hepatic TAG levels ($P < .05$). However, in both male and female LCyp7a1KO mice, VWR significantly increased hepatic TAG levels compared to sedentary LCyp7a1KO mice ($P < .05$). Liver content of the bile acids T-CA, T-αMCA, T-CDCA, and T-DCA were all significantly reduced in LCyp7a1KO mice of both sexes compared to controls (main effect of LCyp7a1KO, $P < .05$, Tables S11 and S12). Moreover, the total bile acid content in the liver, gallbladder, intestines, and feces was significantly lower in LCyp7a1KO mice (main effect of LCyp7a1KO, $P < .05$, Figure 2A-D).

The fraction of new bile acids following ^2H_2O administration was not remarkably different, perhaps due to the much smaller pool sizes in the LCyp7a1KO mice, but the absolute amounts of new bile acids in LCyp7a1KO mice were substantially reduced, consistent with impaired bile acid synthesis (main effect of LCyp7a1KO, $P < .05$, Figure 6D). This reduction was evident across multiple bile acid species, including T-CA, T-αMCA, T-βMCA, T-CDCA, and T-DCA, regardless of sex (main effect of LCyp7a1KO, $P < .05$, Figure 6E-I). Notably, exercise increased T-CA with exercise in male (81.1%) and female (32.8%) control mice (main effect of exercise, $P < .05$, Figure 6E). Furthermore, a significant genotype × VWR interaction revealed that T-DCA synthesis was increased in male control mice that exercised compared to sedentary controls ($P < .05$, Figure 6I). Conversely, a significant genotype × VWR interaction showed that T-CDCA synthesis was reduced in female control mice that exercised ($P < .05$, Figure 6H). These findings indicate that Cyp7a1-mediated bile acid synthesis contributes to the protective effects of exercise against diet-induced hepatic steatosis, as assessed by liver triglyceride levels.

Discussion

Higher aerobic capacity and exercise are known to prevent and treat metabolic diseases, including MASLD,[5–8] respectively. We previously reported that higher aerobic capacity and exercise enhance hepatic gene expression of the bile acid pathway and increase fecal bile acid loss in rodents.[10,11] Moreover, a previous study reported that chronic exercise increased fecal bile acid excretion, accompanied by increased bile acid flow and biliary secretion of cholate-derived bile acids.[12] However, whether hepatic bile acid synthesis is elevated by exercise and if this adaptation plays a critical role in liver metabolism, including the treatment of hepatic steatosis, remained unclear. To assess in vivo bile acid synthesis, we administered ^2H_2O and tracked ^2H incorporation into bile acids by LC-MS/MS detection. These data confirmed that HCR rats have higher bile acid synthesis than LCR rats. Furthermore, 4 weeks of exercise increased hepatic bile acid synthesis in wild-type mice. Consistent with our previous research, both higher aerobic capacity and exercise upregulated *Cyp7a1* gene expression, suggesting that *Cyp7a1* may be essential for the metabolic benefits of both intrinsic exercise capacity and daily physical exercise. For the first time, we also show that the knockout of hepatic *Cyp7a1* reduced bile acid content but increased hepatic steatosis and that it negated the capacity of exercise to lower hepatic steatosis induced by a chronic HFD. Overall, the data show that the regulation of *Cyp7a1* and bile acid synthesis plays a critical role in aerobic capacity and exercise ability in combating MASLD.

Metabolic flexibility, or the capacity to efficiently switch between fuel sources depending on nutrient availability, is crucial for maintaining metabolic health. Impaired metabolic flexibility, such as the inability to properly regulate hepatic lipid synthesis and/or oxidation, is strongly associated with insulin resistance and hepatic steatosis,[41–43] while multiple lines of evidence show that exercise improves metabolic flexibility.[44] Our previous studies demonstrated that HCR rats are protected from HFD-induced insulin resistance and hepatic steatosis and provided evidence of pronounced differences in their whole-body metabolic flexibility, indicated by a superior capacity to upregulate dietary FAO when transitioned to an HFD.[7,45] However, no studies have assessed the capacity of HCR and LCR rat models
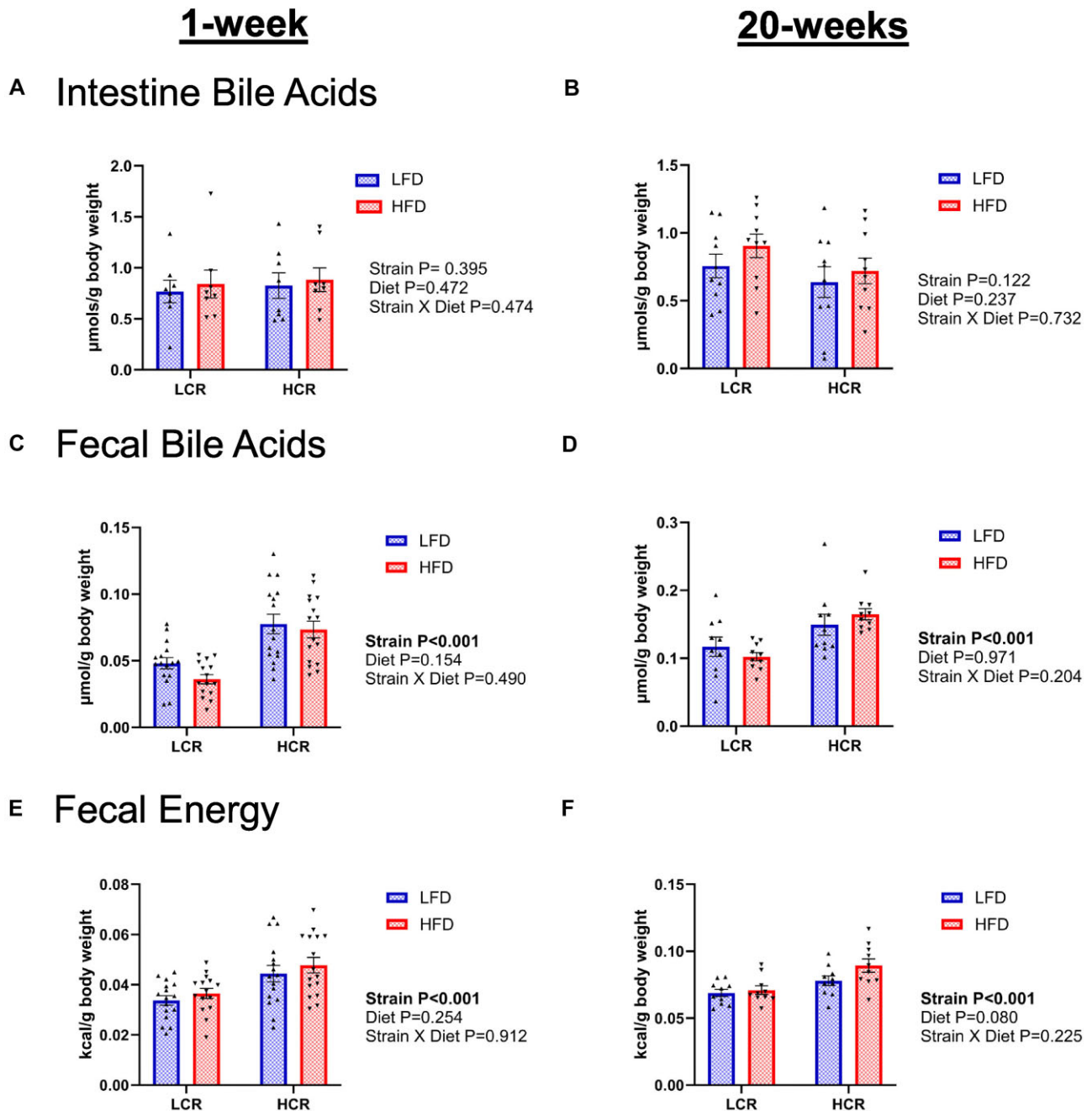
1-week

20-weeks

A Intestine Bile Acids

B

Strain P= 0.395
Diet P=0.472
Strain X Diet P=0.474

Strain P=0.122
Diet P=0.237
Strain X Diet P=0.732

C Fecal Bile Acids

D

Strain P<0.001
Diet P=0.154
Strain X Diet P=0.490

Strain P<0.001
Diet P=0.971
Strain X Diet P=0.204

E Fecal Energy

F

Strain P<0.001
Diet P=0.254
Strain X Diet P=0.912

Strain P<0.001
Diet P=0.080
Strain X Diet P=0.225

Figure 2. Intestinal and fecal bile acid content and fecal energy loss. (A) Intestinal bile acid measurements from rats during the 1-week study ($n = 8$). (B) Intestinal bile acid measurements from rats during the 20-week study ($n = 10$). (C) Fecal bile acid content from rats during the 1-week study ($n = 16$). (D) Fecal bile acid content from rats during the 20-week study ($n = 10$). (E) Fecal energy loss from rats during the 1-week study ($n = 16$). (F) Fecal energy loss from rats during the 20-week study ($n = 10$). Data represented as means $\pm$ SEM.

to moderate DNL in response to nutritional conditions. Consistent with previous research in mice and rats,[8,39] we observed that DNL was stimulated in the fed state and was highest on the carbohydrate-rich LFD. Interestingly, HCR rats displayed a more robust induction of DNL on an LFD, and they suppressed DNL more completely on an HFD compared to LCR rats. The heightened metabolic flexibility of DNL in HCR livers may contribute to their exceptional metabolic profile, such as improved glycemia during high carbohydrate consumption, by increasing the disposal of glucose carbons into lipid stores, or reduced hepatic steatosis during high fat consumption, by activating fat

oxidation with obligate inhibition of DNL. Likewise, similar factors may also play a role in the upregulation of cholesterol and bile acid synthesis in HCR when fed an HFD for 1 week. The shunting of cytosolic acetyl-CoA toward cholesterol and bile acid synthesis may contribute to lower DNL in HCR rats on an HFD. Since sterol synthesis does not require malonyl-CoA, a potent inhibitor of mitochondrial fat transport and oxidation, its increased activity may preserve FAO. Indeed, FAO and mitochondrial respiration are increased in HCR rats,[10,28] which may also facilitate the energy-costly cholesterol and bile acid synthesis pathways. Mechanistic studies will need to be undertaken to
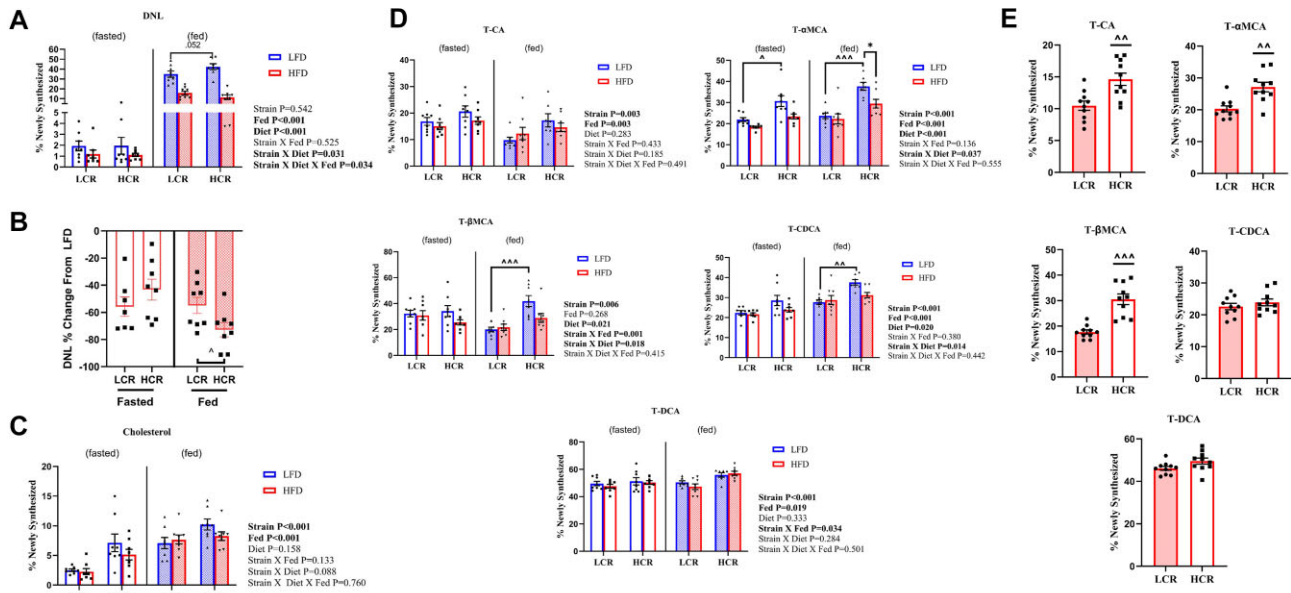
Figure 3. *De novo* lipogenesis (DNL), cholesterol synthesis, and bile acid synthesis. (A) DNL as measured by ^{2}H incorporation into % newly synthesized hepatic palmitate from rats during the 1-week study ($n = 8$). (B) Percent change in DNL from low fat diet (LFD) to high fat diet (HFD) in fasted and fed low capacity runner rats (LCR) and high capacity runner rats (HCR) rats. (C) Cholesterol synthesis as measured by ^{2}H incorporation into % newly synthesized hepatic cholesterol from rats during a 1-week study ($n = 8$). (D) Bile acid synthesis as measured by ^{2}H incorporation into % newly synthesized T-αMCA, T-βMCA, T-CA, T-CDCA, and T-DCA from rats during a 1-week study ($n = 6$-8). (E) Bile acid synthesis as measured by ^{2}H incorporation into % newly synthesized T-αMCA, T-βMCA, T-CA, T-CDCA, and T-DCA from rats during a 20-week study ($n = 10$). Data represented as means $\pm$ SEM. $*$ indicates effect of diet within strain ($*P < .05$, $**P < .01$, $***P < .001$); $^\wedge$ indicates effect of strain within diet ($^\wedge P < .05$, $^{\wedge\wedge}P < .01$, $^{\wedge\wedge\wedge}P < .001$).
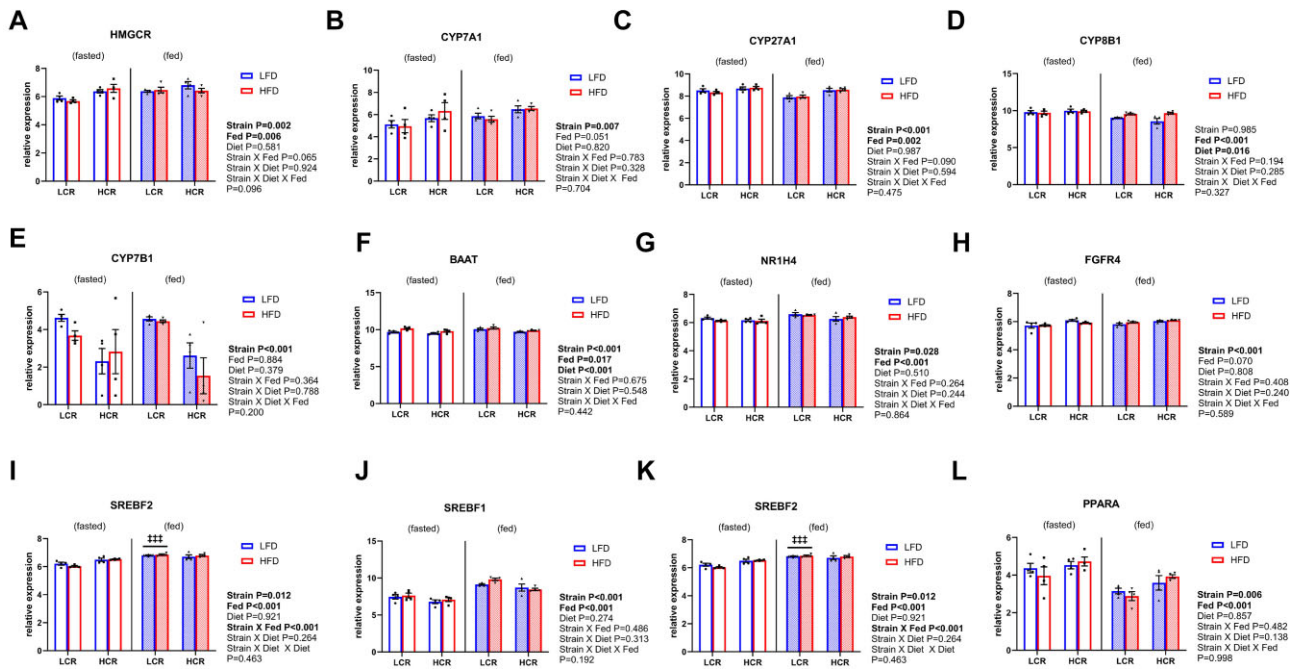
Figure 4. Cholesterol and bile acid synthesis gene expression in high capacity runner rats (HCR) and low capacity runner rats (LCR) rats during a 1-week study. (A) Gene expression for the cholesterol synthesis protein, HMG-CoA reductase (HMGCR). (B) Gene expression for the rate-limiting protein in bile acid synthesis, Cyp7a1. (C) Gene expression for a mitochondrial protein involved in the bile acid synthetic pathway, Cyp27a1. (D) Gene expression for the protein responsible for determining bile acid pool composition, Cyp8b1. (E) Gene expression for a protein in the alternative bile acid synthetic pathway, Cyp7b1. (F) Gene expression for the bile acid-CoA: amino acid N-acyltransferase (BAT) enzyme, which controls the conjugation of bile acids to an amino acid synthesis (BAAT). (G) Gene expression for the hepatic nuclear receptor involved in redundant feedback regulation of bile acids, FXR (NR1H4). (H) Gene expression for a hepatic receptor involved in bile acid feedback from the intestines, FGFR4. (I) Gene expression for a transcription factor that promotes cholesterol synthesis, SREBP-2. (J) Gene expression for a mitochondrial protein involved in the bile acid synthetic pathway, SREBF1. (K) Gene expression for the transcriptional co-activator peroxisome gamma co-activator 1 alpha (PGC1α), a master regulator of mitochondrial biogenesis and genes involved in energy metabolism (PGC1α). (L) Gene expression for a transcription factor that helps regulate fatty acid oxidation in the liver, PPARα (PPARα). Data represented as normalized gene expression values with units as log-transformed counts per million (means $\pm$ SEM; $n = 4$).
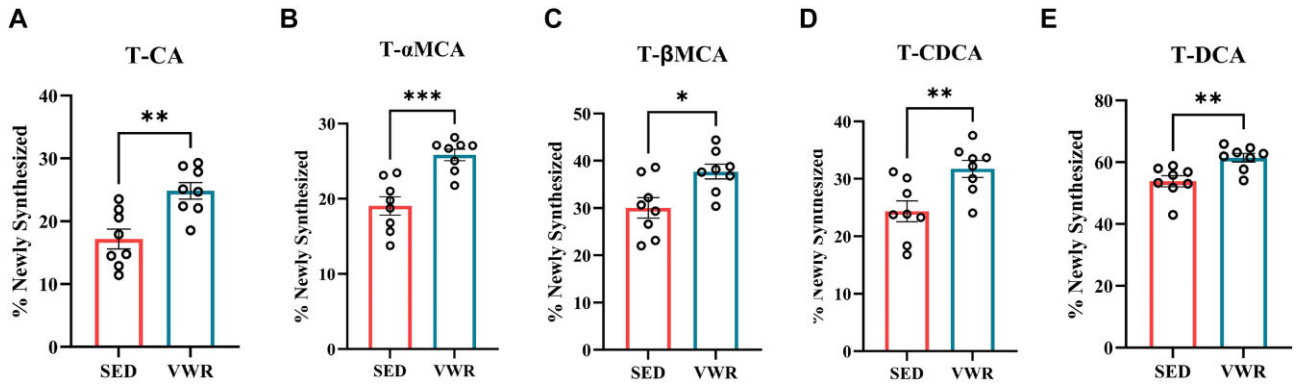
Figure 5. Bile acid synthesis measures in VWR Mice. Data shows bile acid synthesis as measured by ^{2}H incorporation into % newly synthesized. (A) T-CA, (B) T-αMCA, (C) T-βMCA, (D) T-CDCA, and (E) T-DCA. Measurements from mice ($n = 8$) on a high fat diet (HFD) (control) that either remained sedentary (SED) or were given running wheels (VWR) for 4 weeks. Data represented as means ± SEM. $*P < .05$ vs. Sed.
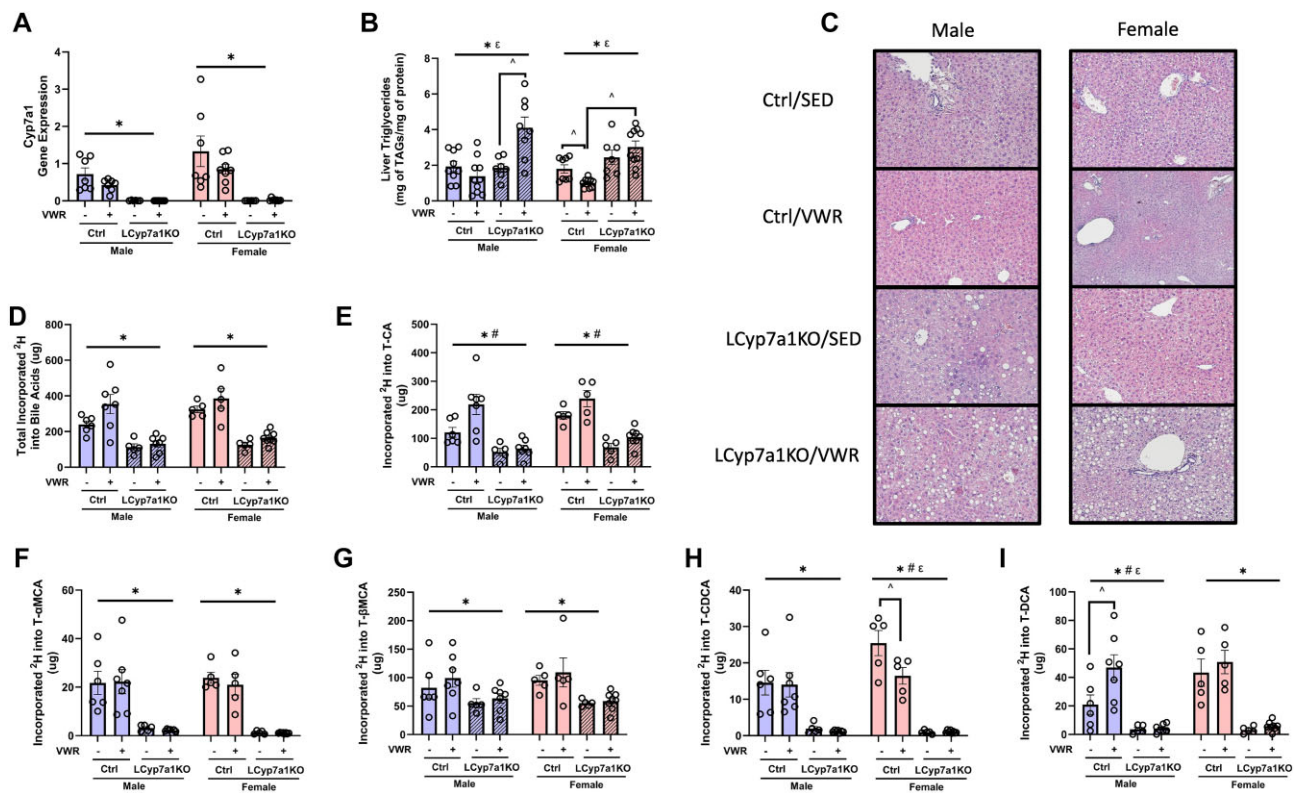

Figure 6. Liver triglyceride and bile acid content in liver-specific Cyp7a1 knockout mice with VWR. (A) Liver Cyp7a1 gene expression. (B) Liver triglyceride content. (C) Representative hematoxylin and eosin stains. (D) Total liver bile synthesis. (E) Liver T-CA bile acid synthesis. (F) Liver T-αMCA bile acid synthesis. (G) Liver T-βMCA bile acid synthesis. (H) Liver T-CDCA bile acid synthesis. (I) Liver T-DCA bile acid synthesis. Data represented as means ± SEM ($n = 6$-10). $*$ Indicates main effect of LCyp7a1KO within sex ($P < .05$), # indicates main effect of VWR within sex ($P < .05$), ε indicates an LCyp7a1KO and VWR interaction within sex, ^ $P < .05$ vs. indicated group.

test the precise link between the activation of bile acid synthesis and increased metabolic flexibility endowed by exercise or intrinsic aerobic capacity.

Our findings reveal a novel link between aerobic capacity, exercise, cholesterol, and bile acid synthesis. Our data shows that HCR rats have enhanced cholesterol synthesis despite maintaining lower serum cholesterol levels, particularly after prolonged HFD feeding. This observation suggests an increased channeling of cholesterol toward bile acid synthesis and fecal excretion in HCR. HCR rats consistently display greater fecal bile acid loss, aligning with previous research in exercising

mice demonstrating elevated bile acid excretion and cholesterol turnover that was previously linked to increased survival and reduced atherosclerotic lesions in LDL-R knockout mice.[12,46] Chronic exercise in mice also upregulates fecal bile acid loss, and tracer studies demonstrate a concomitant increase in bile acid synthesis. These findings are further supported by our previous work in both rodents and humans, where we observed a consistent pattern of increased fecal bile acid levels and/or enhanced expression of hepatic genes involved in cholesterol and bile acid metabolism in response to exercise training.[11,47] Moreover, we showed that improving fitness and reducing body weight with

a diet and exercise intervention in middle-aged, obese women increased a known marker of bile acid synthesis (C4), while also appearing to enhance bile acid feedback regulation.[48] In a previous study, we also compared markers of bile acid metabolism in women with high aerobic capacity vs. moderate aerobic capacity matched for body weight and age.[47] That study did not reveal differences in markers of bile acid synthesis or fecal excretion, likely due to dietary controls that induced unintentional weight loss in high-fit women with very high daily activity levels. However, notably, a marker of bile acid synthesis (C4) and bile acid species were markedly different between high and moderate-fit women during postprandial conditions (OGTT). Glucose and insulin are known regulators of *Cyp7a1* expression and bile acid metabolism.[49] While our data demonstrate that higher aerobic capacity is associated with altered bile acid metabolism both in the fasted and fed states, further research is needed to determine the precise interplay between aerobic capacity, insulin signaling, and bile acid synthesis postprandial regulation.

Collectively, our data in rodents suggest that higher aerobic capacity and exercise promote a shift in cholesterol metabolism toward increased bile acid synthesis and fecal excretion, which appear to facilitate some beneficial effects of exercise on liver health. The primary mechanisms of action by which fitness or exercise leads to greater *Cyp7a1*-mediated bile acid synthesis are unknown but could be linked to higher intestinal motility or less bile acid absorption in the intestines or colon, leading to greater fecal bile acid loss and commensurate increases in bile acid synthesis to maintain homeostasis. However, exercise-induced changes in bile acid metabolism may also result from primary changes in production. A previous study using a crossover within-subject design reported that bile acid levels in the duodenum increased by 10-fold following 30 min of light-intensity exercise vs. sedentary conditions in young men, despite no large difference in total fluid in the duodenum or changes in gall bladder size.[50] This finding could suggest that each bout of exercise increases the production of bile acids, and thus, turnover increases with fecal excretion rising as a result. A newer study found that acute resistance and endurance exercise lowered circulating bile acid levels.[51] However, the effects of acute exercise on bile acid metabolism do not explain the divergent HCR vs. LCR phenotype occurring in rats maintained in a sedentary condition. Exercise and aerobic capacity sensitize hepatic insulin signaling, and activation of the liver with insulin potently upregulates CYP7A1 enzyme expression. Thus, differences in the capacity of insulin to upregulate *Cyp7a1* and bile acid synthesis, in addition to regulating shuttling of acetyl CoA away from DNL toward bile acid synthesis, may also play a role in the capacity of exercise and aerobic capacity to modulate bile acid metabolism.

Differences in insulin sensitivity can also influence bile acid pool composition through the enzyme CYP8B1.[52] *CYP8B1* is an enzyme in the bile acid synthetic pathway responsible for the 12-alpha hydroxylation of bile acids and, therefore, determines the 12-alpha to non-12-alpha hydroxylated bile acid ratio. Insulin action suppresses *CYP8B1* activity; however, insulin resistance causes the ratio of 12-alpha to non-12alpha hydroxylated bile acids to increase.[53] After 20 weeks of an HFD, this ratio was much higher in LCR rats than HCR rats, consistent with our previous observation of worsening metabolic health and reduced insulin signaling in LCR rats on a chronic HFD.[6] There was no significant difference in 12-alpha to non-12-alpha hydroxylated bile acids in the 1-week study, suggesting that initial insulin signaling differences between the strains are not a factor. In contrast, alterations in *Cyp27a1* and *Cyp7b1*, suggest an upregulation of the non-12-alpha hydroxylated bile acid, CDCA, pathway. *Cyp27a1* and *Cyp7b1* are the main regulatory steps in this alternative bile acid synthetic pathway.[54] *Cyp27a1* is localized in mitochondria and is responsible for the side-chain oxidation needed to form bile acids in both the classic and alternative pathways.[55] Hence, the increased expression of *Cyp27a1* in HCR liver likely contributes to a higher overall bile acid synthesis rate and is consistent with our previous finding of higher hepatic *Pgc1α* expression and mitochondrial content in HCR liver.[56] In contrast, greater expression of *Cyp7b1* is a more specific indication that the alternative bile acid pathway is upregulated in LCR liver.

Bile acid synthesis occurs via 2 pathways: classic and alternative. Overexpression of *Cyp7a1*, a rate-limiting enzyme in the classic pathway, attenuates weight gain on an HFD and improves metabolic health, including protecting against hepatic steatosis.[57] Consistent with this, HCR rats and exercise upregulate *Cyp7a1* expression, suggesting a potential role for the classic pathway in preventing and treating hepatic steatosis. However, the relationship between *Cyp7a1* and hepatic steatosis is complex. While *Cyp7a1*-deficient mice from birth exhibit protection from metabolic disorders without altering hepatic steatosis on an HFD.[58] However, bile acids are critical for the digestion and absorption of lipids, and the *Cyp7a1* knockout model reportedly displayed a leanness phenotype due to an inability to digest dietary lipids. In contrast, in this study, the inducible liver-specific *Cyp7a1* knockout model displayed normal weight on the HFD compared to controls and developed increased hepatic steatosis in both sexes. This discrepancy between the knockout methodologies may arise from the reduced capacity of the alternative pathway of *Cyp27a1* to compensate for *Cyp7a1* deficiency in our model or from the fact that we allowed *Cyp7a1* to be functional past a critical developmental window.

Conclusion

In conclusion, this study provides novel insights into the link between aerobic capacity, exercise, bile acid metabolism, and steatosis. Our findings demonstrate that both intrinsic high aerobic capacity and exercise training enhance bile acid synthesis. Elevated bile acid synthesis, driven by *Cyp7a1*, appears critical for the beneficial effects of exercise to treat steatosis induced by an HFD. Importantly, our results identify bile acid synthesis as a key mediator between aerobic capacity, exercise, and hepatic energy metabolism that may also be linked to whole-body metabolism and long-term risk for type 2 diabetes and MASLD, which have shown to be independently linked to aerobic capacity and exercise behavior in human studies. Further investigation is warranted to understand the mechanisms of action by which intrinsic aerobic capacity and exercise lead to greater bile acid synthesis.

Acknowledgments

Author Contributions

Supplementary Material

Supplementary material is available at the *APS Function* online.

Funding

Conflict of Interest

None declared.

Data Availability

All data are found within the manuscript.

References

1. Younossi Z, Anstee QM, Marietti M, et al. Global burden of NAFLD and NASH: trends, predictions, risk factors and prevention. *Nat Rev Gastroenterol Hepatol* 2018;**15**(1):11–20.

2. Friedman SL, Neuschwander-Tetri BA, Rinella M, Sanyal AJ. Mechanisms of NAFLD development and therapeutic strategies. *Nat Med* 2018;**24**(7):908–922.

3. Cuthbertson DJ, Keating SE, Pugh CJA, et al. Exercise improves surrogate measures of liver histological response in metabolic dysfunction-associated steatotic liver disease. *Liver Int* 2024;**44**(9):2368–2381.

4. Fuller KNZ, McCoin CS, Von Schulze AT, Houchen CJ, Choi MA, Thyfault JP. Estradiol treatment or modest exercise improves hepatic health and mitochondrial outcomes in female mice following ovariectomy. *Am J Physiol Endocrinol Metab* 2021;**320**(6):E1020–E1031.

5. Church TS, Kuk JL, Ross R, Priest EL, Biltoff E, Blair SN. Association of cardiorespiratory fitness, body mass index, and waist circumference to nonalcoholic fatty liver disease. *Gastroenterology* 2006;**130**(7):2023–2030.

6. Morris EM, Meers GME, Koch LG, et al. Aerobic capacity and hepatic mitochondrial lipid oxidation alters susceptibility for chronic high-fat diet-induced hepatic steatosis. *Am J Physiol Endocrinol Metab* 2016;**311**(4):E749–E760.

7. Noland RC, Thyfault JP, Henes ST, et al. Artificial selection for high-capacity endurance running is protective against high-fat diet-induced insulin resistance. *Am J Physiol Endocrinol Metab* 2007;**293**(1):E31–41.

8. Morris EM, Jackman MR, Johnson GC, et al. Intrinsic aerobic capacity impacts susceptibility to acute high-fat diet-induced hepatic steatosis. *Am J Physiol Endocrinol Metab* 2014;**307**(4):E355–364.

9. Syed-Abdul MM. Lipid metabolism in metabolic-associated steatotic liver disease (MASLD). *Metabolites*. 2023;**14**(1):12.

10. Kugler BA, Cao X, Wenger M, et al. Divergence in aerobic capacity influences hepatic and systemic metabolic adaptations to bile acid sequestrant and short-term high-fat/sucrose feeding in rats. *Am J Physiol-Regul, Integr Comp Physiol* 2023;**325**(6):R712–R724.

11. Stierwalt HD, Morris EM, Maurer A, et al. Rats with high aerobic capacity display enhanced transcriptional adaptability and upregulation of bile acid metabolism in response to an acute high-fat diet. *Physiol Rep* 2022;**10**(15), e15405. https://doi.org/10.14814/phy2.15405.

12. Meissner M, Lombardo E, Havinga R, Tietge UJF, Kuipers F, Groen AK. Voluntary wheel running increases bile acid as well as cholesterol excretion and decreases atherosclerosis in hypercholesterolemic mice. *Atherosclerosis* 2011;**218**(2):323–329.

13. Watanabe M, Morimoto K, Houten SM, et al. Bile acid binding resin improves metabolic control through the induction of energy expenditure. *PLoS One* 2012;**7**(8):e38286.

14. Watanabe M, Houten SM, Mataki C, et al. Bile acids induce energy expenditure by promoting intracellular thyroid hormone activation. *Nature* 2006;**439**(7075):484–489.

15. Qi Y, Jiang C, Cheng J, et al. Bile acid signaling in lipid metabolism: metabolomic and lipidomic analysis of lipid and bile acid markers linked to anti-obesity and anti-diabetes in mice. *Biochim Biophys Acta* 2015;**1851**(1):19–29.

16. Puri P, Baillie RA, Wiest MM, et al. A lipidomic analysis of nonalcoholic fatty liver disease. *Hepatology* 2007;**46**(4):1081–1090.

17. Van Rooyen DM, Larter CZ, Haigh WG, et al. Hepatic free cholesterol accumulates in obese, diabetic mice and causes nonalcoholic steatohepatitis. *Gastroenterology* 2011;**141**(4):1393–1403.e1395.

18. Previs SF, Mahsut A, Kulick A, et al. Quantifying cholesterol synthesis in vivo using (2)H(2)O: enabling back-to-back studies in the same subject. *J Lipid Res* 2011;**52**(7):1420–1428.

19. Lee WN, Bassilian S, Guo Z, et al. Measurement of fractional lipid synthesis using deuterated water (2H2O) and mass isotopomer analysis. *Am J Physiol* 1994;**266**(3):E372–383.

20. Fu X, Deja S, Fletcher JA, et al. Measurement of lipogenic flux by deuterium resolved mass spectrometry. *Nat Commun* 2021;**12**(1):3756.

21. Castro-Perez J, Previs SF, McLaren DG, et al. In vivo D2O labeling to quantify static and dynamic changes in cholesterol and cholesterol esters by high resolution LC/MS. *J Lipid Res* 2011;**52**(1):159–169.

22. Lambert JE, Ryan EA, Thomson AB, Clandinin MT. De novo lipogenesis and cholesterol synthesis in humans with long-standing type 1 diabetes are comparable to non-diabetic individuals. *PLoS One* 2013;**8**(12):e82530.

23. Diraison F, Pachiaudi C, Beylot M. In vivo measurement of plasma cholesterol and fatty acid synthesis with deuterated water: determination of the average number of deuterium atoms incorporated. *Metabolism* 1996;**45**(7): 817–821.

24. Jones PJ. Use of deuterated water for measurement of short-term cholesterol synthesis in humans. *Can J Physiol Pharmacol* 1990;**68**(7):955–959.

25. Jones PJ, Ausman LM, Croll DH, Feng JY, Schaefer EA, Lichtenstein AH. Validation of deuterium incorporation against sterol balance for measurement of human cholesterol biosynthesis. *J Lipid Res* 1998;**39**(5):1111–1117.

26. Lee WN, Bassilian S, HO A, et al. In vivo measurement of fatty acids and cholesterol synthesis using D2O and mass isotopomer analysis. *Am J Physiol* 1994;**266**(5): E699–708.

27. Kempen HJ, Vos Van Holstein M, De Lange J. Bile acids and lipids in isolated rat hepatocytes. II. Source of cholesterol used for bile acid formation, estimated by incorporation of tritium from tritiated water, and by the effect of ML-236B. *J Lipid Res* 1983;**24**(3):316–323.

28. Thyfault JP, Rector RS, Uptergrove GM, et al. Rats selectively bred for low aerobic capacity have reduced hepatic mitochondrial oxidative capacity and susceptibility to hepatic steatosis and injury. *J Physiol* 2009;**587**(8): 1805–1816.

29. Koch LG, Britton SL. Artificial selection for intrinsic aerobic endurance running capacity in rats. *Physiol Genomics* 2001;**5**(1):45–52.

30. Morris EM, Noland RD, Ponte ME, et al. Reduced liver-specific PGC1a increases susceptibility for short-term diet-induced weight gain in male mice. *Nutrients* 2021;**13**(8):2596.

31. Wankhade UD, Zhong Y, Kang P, et al. Enhanced offspring predisposition to steatohepatitis with maternal high-fat diet is associated with epigenetic and microbiome alterations. *PLoS One* 2017;**12**(4):e0175675.

32. Hasan MN, Chen J, Matye D, et al. Combining ASBT inhibitor and FGF15 treatments enhances therapeutic efficacy against cholangiopathy in female but not male Cyp2c70 KO mice. *J Lipid Res* 2023;**64**(3):100340.

33. Kister B, Viehof A, Rolle-Kampczyk U, et al. A physiologically based model of bile acid metabolism in mice. *iScience* 2023;**26**(10):107922.

34. Zheng C, Wang L, Zou T, et al. Ileitis promotes MASLD progression via bile acid modulation and enhanced TGR5 signaling in ileal CD8(+) T cells. *J Hepatol* 2024;**80**(5): 764–777.

35. Reiter S, Dunkel A, Dawid C, Hofmann T. Targeted LC-MS/MS profiling of bile acids in various animal tissues. *J Agric Food Chem* 2021;**69**(36):10572–10580.

36. Jäntti SE, Kivilompolo M, Öhrnberg L, et al. Quantitative profiling of bile acids in blood, adipose tissue, intestine, and gall bladder samples using ultra high performance liquid chromatography-tandem mass spectrometry. *Anal BioanalChem* 2014;**406**(30):7799–7815.

37. Han J, Liu Y, Wang R, Yang J, Ling V, Borchers CH. Metabolic profiling of bile acids in human and mouse blood by LC-MS/MS in combination with phospholipid-depletion solid-phase extraction. *Anal Chem* 2015;**87**(2):1127–1136.

38. Brunengraber H, Kelleher JK, Des Rosiers C. Applications of mass isotopomer analysis to nutrition research. *Annu Rev Nutr* 1997;**17**(1):559–596.

39. Duarte JA, Carvalho F, Pearson M, et al. A high-fat diet suppresses de novo lipogenesis and desaturation but not elongation and triglyceride synthesis in mice. *J Lipid Res* 2014;**55**(12):2541–2553.

40. Kugler BA, Thyfault JP, McCoin CS. Sexually dimorphic hepatic mitochondrial adaptations to exercise: a mini-review. *J Appl Physiol* 2023;**134**(3):685–691.

41. Greenberg AS, Coleman RA, Kraemer FB, et al. The role of lipid droplets in metabolic disease in rodents and humans. *J Clin Invest* 2011;**121**(6):2102–2110.

42. Deivanayagam S, Mohammed BS, Vitola BE, et al. Nonalcoholic fatty liver disease is associated with hepatic and skeletal muscle insulin resistance in overweight adolescents. *Am J Clin Nutr* 2008;**88**(2):257–262.

43. Korenblat KM, Fabbrini E, Mohammed BS, Klein S. Liver, muscle, and adipose tissue insulin action is directly related to intrahepatic triglyceride content in obese subjects. *Gastroenterology* 2008;**134**(5): 1369–1375.

44. Thyfault JP, Rector RS. Exercise combats hepatic steatosis: potential mechanisms and clinical implications. *Diabetes* 2020;**69**(4):517–524.

45. Morris EM, Meers GME, Ruegsegger GN, et al. Intrinsic high aerobic capacity in male rats protects against diet-induced insulin resistance. *Endocrinology* 2019;**160**(5): 1179–1192.

46. Meissner M, Havinga R, Boverhof R, Kema I, Groen AK, Kuipers F. Exercise enhances whole-body cholesterol turnover in mice. *Med Sci Sports Exerc* 2010;**42**(8): 1460–1468.

47. Maurer A, Ward JL, Dean K, et al. Divergence in aerobic capacity impacts bile acid metabolism in young women. *J Appl Physiol (1985)* 2020;**129**(4):768–778.

48. Mercer KE, Maurer A, Pack LM, et al. Exercise training and diet-induced weight loss increase markers of hepatic bile acid (BA) synthesis and reduce serum total BA concentrations in obese women. *Am J Physiol Endocrinol Metab* 2021;**320**(5):E864–E873.

49. Li T, Francl JM, Boehme S, et al. Glucose and insulin induction of bile acid synthesis. *J Biol Chem* 2012;**287**(3): 1861–1873.

50. Simko V, Kelley RE. Effect of physical exercise on bile and red blood cell lipids in humans. *Atherosclerosis* 1979;**32**(4):423–434.

51. Morville T, Sahl RE, Trammell SAJ, et al. Divergent effects of resistance and endurance exercise on plasma bile acids, FGF19, and FGF21 in humans. *JCI Insight* 2018;**3**(15):e122737. https://doi.org/10.1172/jci.insight.122737.

52. Haeusler RA, Pratt-Hyatt M, Welch CL, Klaassen CD, Accili D. Impaired generation of 12-hydroxylated bile acids links hepatic insulin signaling with dyslipidemia. *Cell Metab* 2012;**15**(1):65–74.

53. Haeusler RA, Astiarraga B, Camastra S, Accili D, Ferrannini E. Human insulin resistance is associated with increased plasma levels of 12alpha-hydroxylated bile acids. *Diabetes* 2013;**62**(12):4184–4191.

54. Pandak WM, Kakiyama G. The acidic pathway of bile acid synthesis: not just an alternative pathway(☆). *Liver Res* 2019;**3**(2):88–98.

55. Björkhem I. Mechanism of degradation of the steroid side chain in the formation of bile acids. *J Lipid Res* 1992;**33**(4):455–471.

56. Thyfault JP, Morris EM. Intrinsic (Genetic) aerobic fitness impacts susceptibility for metabolic disease. *Exerc Sport Sci Rev* 2017;**45**(1):7–15.

57. Li T, Owsley E, Matozel M, Hsu P, Novak CM, Chiang JYL. Transgenic expression of cholesterol 7α-hydroxylase in the liver prevents high-fat diet-induced obesity and insulin resistance in mice. *Hepatology* 2010;**52**(2):678–690.

58. Ferrell JM, Boehme S, Li F, Chiang JYL. Cholesterol 7α-hydroxylase-deficient mice are protected from high-fat/high-cholesterol diet-induced metabolic disorders. *J Lipid Res* 2016;**57**(7):1144–1154.